ELSEVIER

Journal of Chromatography B, 743 (2000) 151–167

JOURNAL OF CHROMATOGRAPHY B

www.elsevier.com/locate/chromb

Diffusion of lysozyme in gels and liquids A general approach for the determination of diffusion coefficients using holographic laser interferometry

Charlotte Mattisson[a], Philippe Roger[b], Bengt Jönsson[c], Anders Axelsson[a,*], Guido Zacchi[a]

[a]*Department of Chemical Engineering 1, Lund University, P.O. Box 124, SE-221 00 Lund, Sweden*
[b]*Institut National de la Recherche Agronomique, Nantes Cedex, France*
[c]*Department of Physical Chemistry 1, Lund University, Lund, Sweden*

Abstract

A study on diffusion measurements of the protein lysozyme in liquids and agarose gels, at different pH and ionic strengths, has been performed using holographic laser interferometry. The measurements showed that the diffusive flux was very dependent on pH and ionic strength when the protein was not at its isoelectric point or when the charge of the lysozyme molecules was not screened by ions in the solution. Evaluation of the experimental data with Fick's law, resulted in diffusion coefficients for lysozyme that are strongly dependent on pH and ionic strength. Evaluation of the experimental data using a more general transport model, based on chemical potential gradients instead of concentration gradients resulted in lysozyme diffusion coefficients that are independent of pH and ionic strength. The chemical potential was estimated by using the Poisson–Boltzmann equation. © 2000 Elsevier Science B.V. All rights reserved.

Keywords: Diffusion coefficients; Holographic laser interferometry; Lysozome

1. Introduction

The diffusive properties of proteins are important in several situations for example in chromatography. The interaction with the gel adsorbent and the interaction with the solvent influence the separation very much. This paper treats this problem in order to give an understanding of how to describe the diffusive properties as well as how to experimentally verify them.

Proteins are charged macromolecules that consist of a number of amino acids linked together by peptide bonds. The surface of a protein molecule is in most cases covered with weak acid and basic groups, while the interior of a protein is more hydrophobic. The pH sets the degree of protolysis and thus the degree of ionisation of the surface groups and thereby the net charge of the protein. In acid solutions, proteins are strongly positive, but as the pH increases the net charge decreases and becomes equal to zero at the isoelectric point. At this pH the positive and negative charges cancel. If the pH increases further, the protein net charge becomes negative [1,2].

A characteristic property of macromolecules in solution is the balance between different attractive and repulsive interactions. The repulsive interactions

*Corresponding author. Fax: +46-46-222-4526.
E-mail address: anders.axelsson@kat.lth.se (A. Axelsson)

0378-4347/00/$ – see front matter © 2000 Elsevier Science B.V. All rights reserved.
PII: S0378-4347(99)00535-6

are often due to electrostatic forces, while van der Waals interactions are the dominating attractive forces. If salt is added to a solution with charged macromolecules, the electrostatic repulsion between the charged molecules decreases because the salt ions screen the charged macromolecules from each other. This makes it important to understand the electrostatic interactions between charged macromolecules since a solution of macromolecules can change its properties significantly due to changes in pH, ionic strength and concentration.

Several papers in the literature report liquid diffusion coefficients for proteins that vary depending on ionic strength, pH and protein concentration [3–7]. The same behaviour has been reported to occur in amylopectin gels [8]. In all the papers mentioned above a high diffusion coefficient appear at low ionic strength and a variation with protein concentration is also observed. If the ionic strength is increased the diffusion rate decreases and becomes less dependent on protein concentration. Wesselingh and Krishna [2] and Leaist [5] explain the observed high diffusion coefficients at low ionic strength as an effect of electroneutrality conditions. When charged proteins diffuse with small mobile counterions, charge separation is prevented since the diffusion process induces an electric field that slows down the small counterions and speeds up the protein ions. When the concentration of small counterions increases, they replace the protein ions and the diffusion rate for the protein decreases. This is a result of the higher mobility of the smaller counterions.

The aim of this study is to present an alternative way, compared to Fick's law, to describe the diffusive mass flux for systems with charged macromolecules. This is done in order to avoid diffusion coefficients that are strongly dependent on pH, concentration or ionic strength. This can be achieved by using a general transport model where a chemical potential gradient is used as a driving force, instead of a concentration gradient as in Fick's law. Computer simulations based on the diffusive flow in a chemical potential gradient, here denoted the general model, were performed to study how ionic strength and pH affect the diffusive flux in gels and liquids.

Experiments were performed using holographic laser interferometry (HLI). This method presents an elegant way to study the whole concentration profile in the gel as well as in the liquid. Furthermore, this type of method is a prerequisite for the present study in which the concentration profiles are used to understand and describe the diffusive properties. HLI has earlier been shown to be a suitable method for diffusion studies in gels and liquids for both small and large solutes [9–19]. Partition coefficients and diffusion coefficients for lysozyme in both liquids and agarose gels, at different pH and ionic strength were determined. The experimental data were evaluated using both Fick's law and the general model.

2. Theory

2.1. Diffusion theory

The thermodynamic quantity that governs spontaneous molecular transport is the gradient of the chemical potential, μ. According to chemical thermodynamics the change of the chemical potential in the x-direction can be regarded as an effective force, $\mathbf{F}_t$

$$\mathbf{F}_t = -\frac{\partial \mu}{\partial x} \tag{1}$$

A diffusive flux is the response of the molecules to this effective force. If the flux of material, J, is assumed to be proportional to the effective force, $\mathbf{F}_t$, then the flux can be described by [20]

$$J = -\frac{D}{RT} c \frac{\partial \mu}{\partial x} \tag{2}$$

where D is the diffusion coefficient, R the universal gas constant, T the temperature and c the concentration. This equation describes a time-independent flux, i.e., diffusive flux down a chemical potential gradient. For an ideal solution Eq. (2) is identical to Fick's law. Equations for time-dependent diffusion processes can be derived using Eq. (2)

$$\frac{\partial c(x,t)}{\partial t} = \frac{D}{RT} c \frac{\partial}{\partial x}\left(\frac{\partial \mu(x,t)}{\partial x}\right) \tag{3}$$

The chemical potential, μ_i, for a solution with compound i, consists of contributions from pressure (P), activity (a_i), temperature (T) and long-range electrostatic interactions ($\mu_{i,el}$) [2] and is given by:

$$\mu_i = \mu_i^o + V_i(P - P^o) + RT \ln a_i - S_i(T - T^o) + \mu_{i,el} \quad (4)$$

For a solution at constant pressure and temperature and with negligible long electrostatic interactions the chemical potential, μ, is

$$\mu = \mu^o + RT \ln a \quad (5)$$

For ideal solutions at constant pressure and temperature, the activity, a, in Eq. (5) may be replaced by the concentration, c. Eq. (6) is obtained by derivation of Eq. (5) where the activity has been substituted by the concentration

$$\frac{\partial \mu}{\partial x} = RT \frac{1}{c} \frac{\partial c}{\partial x} \quad (6)$$

Substituting Eq. (6) into Eq. (3) results in the familiar Fick's second law:

$$\frac{\partial c(x,t)}{\partial t} = D \frac{\partial^2 c(x,t)}{\partial x^2} \quad (7)$$

This is the most common way to describe time-dependent diffusion. For ideal systems it often gives a good agreement between theoretical predictions and experimental results. However, as can be seen above it is based on the assumption that the activity can be replaced by the concentration and that there are no pressure, temperature or electrostatic interaction gradients. This is a good assumption for ideal systems but for systems with charged macromolecules it is not valid, due to the electrostatic interactions in these systems.

The simplest case when discussing the interaction between charged particles is when only two charges interact with each other. According to Coulomb's law the force, $\mathbf{F}_t$, between the two charges, q_1 and q_2, depends on the magnitude of each charge and the distance, r, between them.

$$\mathbf{F}_t = \frac{1}{4\pi\varepsilon_0} \frac{q_1 q_2}{r^2} \quad (8)$$

In a solution with macromolecules, the main factors influencing the strength of the interaction forces between the macromolecules are the size of the macromolecules, the charge of each molecule and the molecular concentration. These interactions can be reduced by adding ions in the form of salts to the solution. The salt ions will then screen the macromolecules from each other and thereby lower the electrostatic interaction in the solution. Proteins in solution are charged macromolecules and a protein solution with low ionic strength can be highly non-ideal. This means that substituting activity for concentration and not including electrical potential when describing a diffusive flux of charged proteins, can be a rather poor approach. However, at moderate protein concentrations with high ionic strength, the system normally behaves as an ideal system and substituting activity with concentration is acceptable [3,5–8,19].

The chemical potential for protein solutions, including electrostatic contributions, can be calculated by using the Poisson–Boltzmann equation (Eq. 9) to describe the electrostatics. This is conveniently done by applying the PBCell model [21,22]. The electrostatic potential $\Psi(r)$ is given by:

$$\nabla^2 \Psi(\vec{r}) = -\frac{F}{\varepsilon_0 \varepsilon_r} \sum_j z_j c_j(\text{bulk}) \exp\left(\frac{-F z_j \Psi(\vec{r})}{RT}\right) \quad (9)$$

In Eq. (9) F is Faraday's constant, ε_o is the vacuum permittivity, ε_r is the dielectric constant for the solvent, z_j is the charge number of the ions, c_j is the bulk concentration of the ions and $\Psi(r)$ is the electrostatic potential. By calculating the chemical potential of a lysozyme molecule for different lysozyme concentrations, it is possible to obtain a function that describes how the chemical potential varies with concentration, $\mu(c_{\text{lysozyme}})$. This function can then be substituted into Eq. (3).

3. Experimental

3.1. Gel preparation

Agarose gels of 4.0% (w/w) (Agarose IEF, kindly provided by Pharmacia Biotech, Uppsala, Sweden) were prepared by weighing agarose powder and degassed distilled water into screw-capped tubes with teflon-protected seals. The agarose was suspended in water by gently shaking until a homogeneous suspension was obtained and dissolved by heating in boiling water with occasional shaking during 10–15 min. Direct observation ensured that

the contents of the tubes were clear. The hot solution was then transferred into a diffusion cell using a preheated syringe.

The diffusion cell, which can be seen in Fig. 1, was made of Plexiglass. Gelification occurred after approximately 20 min, the sol–gel transition was followed by a change from transparent to a slightly milky white colour. The gels were then carefully pushed out of the diffusion cell and the lower part was sliced off with a razor blade in order to obtain a plane surface. The gels were equilibrated (for at least 24 h) and stored in the same solvent as the one used for the protein solutions.

3.2. Protein solution preparation

The lysozyme (L-6876, Lot 65H7025) was supplied by Sigma (St. Louis, MO, USA). A 1% lysozyme solution (10 mg/ml) was obtained by dissolving the corresponding amount of dry lysozyme powder in either distilled water or in 0.1 *M* NaCl. The pH in the lysozyme solution was adjusted to 4, 5.6 or 11 by adding small volumes of either HCl or NaOH. To minimise the amount of salt ions present in the lysozyme solution no buffer was used. The protein solutions were used immediately after preparation, and the pH was also measured after the diffusion experiment, in order to check if the pH had altered during the experiment. Protein characteristics for lysozyme are presented in Table 1 and 2.

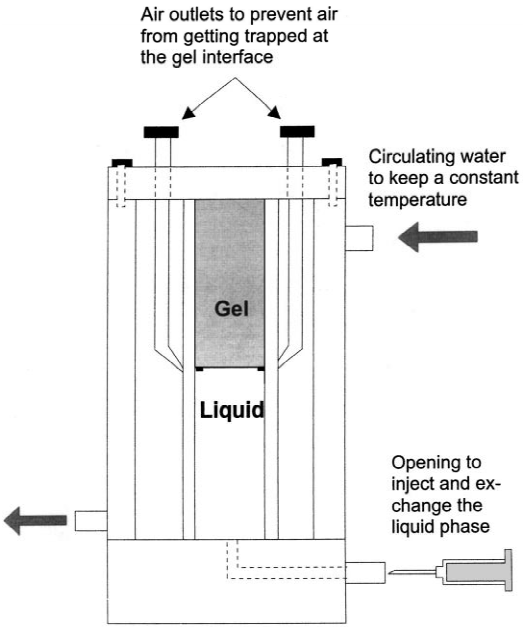

Fig. 1. Schematic illustration of the diffusion cell used in the holographic laser interferometry experiments.

Table 1
Lysozyme characteristics

M_w (g/mol)	Stokes radius (nm)	Isoelectric point	D_{liq}[a] (10^{-11} m^2/s)
14 600	1.9	11.2[b]	13.7[c], 12.26[d], 11.5[e], 13.45[f], 12.80[g]

[a] Values adjusted to 25°C according to Stokes–Einsteins equation.
[b] [22].
[c] [4] Dynamic light scattering.
[d] [28] Analytical SPLITT fractionation.
[e] [29] Dynamic light scattering.
[f] [30] FFF.
[g] [24] Chromatography.

3.3. Refractive index measurements

The refractive index for lysozyme solutions, with and without NaCl, in the range 0–10 mg/ml protein was measured on an RFM81 Multiscale Refractometer (Bellingham & Stanley, Kent TN2 3EY, UK) at 25°C. The refractive index was found to vary linearly with concentration. The value of d*n*/d*c* was 0.196 ml/g when no extra salt was added and 0.165 ml/g in a 0.1 *M* NaCl solution.

3.4. Diffusion measurements using HLI

The experimental procedure for HLI was the same as described earlier by Mattisson et al. [14], although the experimental set-up was slightly modified. The

Table 2
Charge of lysozyme at different pH

pH	Lysozyme charge number[a]	
	5 m*M* NaCl	0.1 *M* NaCl
4	12	13
5.6	10	10.5
11	1	1

[a] [22].

primary difference was that the diffusion cell used was especially designed for diffusion studies of macromolecules. In this diffusion cell the gel was placed at the top of the diffusion cell and the liquid below the gel. This was necessary to avoid convection in the liquid phase. Small supports prevented the gel from sliding down (Fig. 1). The gel was introduced into the diffusion cell and carefully pushed down until it reached the support. The diffusion cell was sealed with a lid to prevent evaporation and then placed into a transparent Plexiglass holder. A solvent solution was introduced into the lower part of the diffusion cell by a syringe connected to an inlet at the lower part of the Plexiglass holder. Two outlets placed on each side of the diffusion cell immediately below the small supports and connected to the outside of the Plexiglass holder via flexible tubings were necessary to prevent air bubbles from getting trapped at the interface when the solvent solution was introduced.

All experiments were performed at 25°C. At the time of exposure the solution under the gel was in equilibrium with the gel. After the exposure the holographic plate was processed and then reinserted in exactly the same position as at the time of exposure. The diffusion process was started by carefully replacing the liquid that was in equilibrium with the gel with a protein solution. This was done by using a syringe connected to the outlet of the diffusion cell. The start concentration of lysozyme was 10 mg/ml in the liquid phase and 0 mg/ml in the gel phase for all experiments.

3.5. Partition coefficients from HLI measurements

The system studied consists of a gel phase (1) and a liquid phase (2) with the interface at $x=0$ (Fig. 2).

Initially at $t=0$, the protein concentration is zero in the gel phase (C_{10}) and is uniform in the liquid phase (C_{20}). The gel diffusion coefficient for a protein in the gel phase is D_g and in the liquid phase D_2. Both phases are considered to be semi-infinite. The boundary conditions at the interface $x=0$ can be written

$$k = \frac{C_{1,\mathrm{eq}}}{C_{2,\mathrm{eq}}} \quad (x = 0) \tag{10}$$

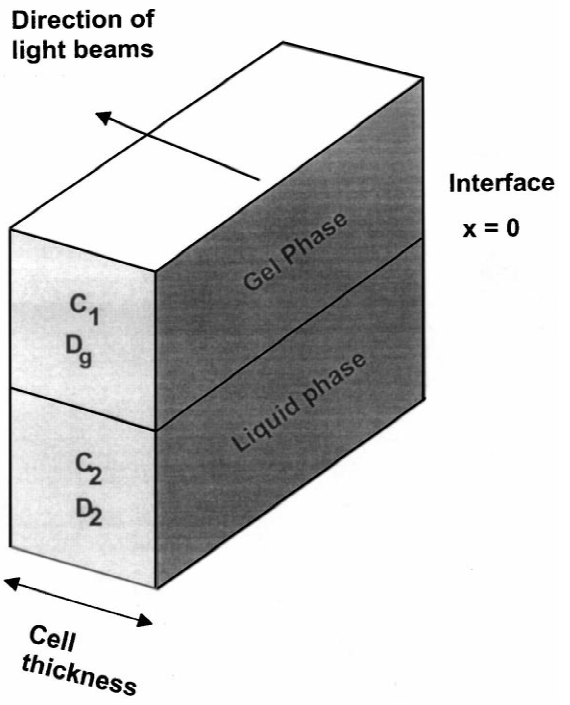

Fig. 2. Schematic illustration of the studied system consisting of a gel phase (1) and a liquid phase (2). The distance from the gel–liquid interface is x. C_1 and C_2 denote the concentration of lysozyme in the gel phase and liquid phase, respectively. D_g is the gel diffusion coefficient for lysozyme in the gel phase, and D_2 is the diffusion coefficient for lysozyme in the liquid phase.

$$C_1 D_g \frac{\partial \mu_1}{\partial x} = C_2 D_2 \frac{\partial \mu_2}{\partial x} \quad (x = 0) \tag{11}$$

where k is the partition coefficient and $C_{1,\mathrm{eq}}$, $C_{2,\mathrm{eq}}$ are the equilibrium concentrations in the gel and liquid phase, respectively. The second boundary condition, Eq. (11), implies that there is no accumulation of protein at the interface.

If the two boundary conditions above are used to solve Fick's second law (using concentration gradients instead of chemical potential gradients) it can be shown that the concentration at the interface, $x=0$, remains constant during the diffusion process [23]. As diffusion progresses, the concentration in the x direction will change in both phases. The refractive index along the cell will thus change and result in dark and light interference fringes in both phases. The parameter that sets the total number of fringes in each phase is the concentration difference

between the interface ($x=0$) and the unaffected part ($x=\infty$), ΔC_{tot} where

$$\Delta C_{tot} = C_{l=\infty} - C_{int} \quad (12)$$

The concentration in the unaffected part of the phase, $C_{l=\infty}$, is the same as the start concentration, C_{10} or C_{20}, during the whole experiment. The concentration at the interface, C_{int}, in each phase is equal to the equilibrium concentration in each phase, $C_{1,eq}$ or $C_{2,eq}$, according to the first boundary condition [23]. $C_{1,eq}$ and $C_{2,eq}$ can be estimated from the interference pattern.

The change in refractive index that is necessary to produce a dark or light interference fringe is:

$$\Delta n = \frac{\lambda}{2b} \quad (13)$$

where λ is the wave length, 632.8 nm, of the used light source and b the thickness of the diffusion cell. The total number of fringes (dark and light) in a phase gives the total change in refractive index between the interface and $x=\infty$. If the relationship between concentration and refractive index is known, it is possible to obtain ΔC_{tot}, Then using Eq. (12) it is possible to obtain $C_{1,eq}$, $C_{2,eq}$ and finally the partition coefficient using Eq. (10). The refractive index for agarose gel containing x mg/ml protein is assumed to be the same as the refractive index for a solution with x mg/ml protein plus a constant. The constant is the contribution from the polymer fibres in the gel and is assumed to be independent of protein concentration.

When obtaining the partition coefficient according to the method described above, a maximum deviation from the best estimated partition coefficient can be estimated. The best estimated value is based on the best possible estimation of the total number of fringes (dark and light) in each phase. The maximum error in the estimation of the total number of fringes is normally half a fringe in each phase. Assuming that the best estimation of the total number of fringes in each phase is wrong by half a fringe it is possible to obtain a maximum and minimum value of the partition coefficient. These values can then be used to describe the interval within the best estimation which may vary.

The evaluation and interpretation of experimental interference patterns obtained with HLI (to obtain concentration profiles) was the same as described by Mattisson et al. [14]

4. Simulation study

Simulations based on the general model (Eq. 3) were performed to study how pH and ionic strength affected concentration profiles in a system identical to the one studied experimentally. The liquid diffusion coefficient, D_{liq}, and the gel diffusion coefficient, D_g, were set to 12.80×10^{-11} and 6.3×10^{-11} m^2/s, respectively. The partition coefficient was set to 0.86. These are experimental values obtained for lysozyme by chromatography, in a Sephadex G-200 gel (2.7%, w/v) by Vonk [24].

All concentration profiles were calculated to represent the situation after 2 h of diffusion time. The interface concentrations in each phase were obtained from the condition that the flux in the gel phase and the liquid phase should be the same.

A computer program, PBCell, was used to calculate chemical potentials in the concentration interval 0–12 mg/ml lysozyme. PBCell solves the Poisson–Boltzmann equation numerically for different protein geometries, concentrations and ionic strengths [21,22].

Input parameters to PBCell are presented in Table 3.

Table 3
Input parameters to PBCell [21,22,31]

Cell shape	Spherical
Radius of the charged interface	19 Å
Volume fraction of region 1	Interval between 0.0148–0.00061
Area/surface charge	4540/charge number $Å^2$ (charge number varies with pH)
Charge number salt 1	+1/−1
Bulk conc. of cation 1	5 or 100 m*M*
Charge number salt 2	+1/−1
Bulk conc. of cation 2	0 m*M*
Temp. in the system	298 K
Hamaker constant	6E-21 J
Surface energy	0.018 J/m^2

5. Result

5.1. Simulation results

All simulated concentration profiles are determined for conditions after 2 h of diffusion using the general model. Fig. 3 shows simulated concentration profiles, based on Eq. (3), at pH 4 and 11 for a low ionic strength of 5 m*M* NaCl. At pH 4 the chemical potential is high since lysozyme is highly charged. This results in a high driving force and thereby a high diffusive flux. At pH 11 lysozyme is very close to its isoelectric point and has a very low charge and hence the chemical potential and the diffusive flux will be lower than at pH 4. The effect is more pronounced in the liquid phase than in the gel phase, since the concentration in the liquid phase is higher than in the gel phase.

Fig. 4 shows simulated concentration profiles, based on Eq. (3), at pH 4 and 11 at an ionic strength of 0.1 *M* NaCl. The difference between the profiles is smaller than at the low ionic strength. This is due to increased electrostatic screening of the charged lysozyme molecules by the added salt.

Fig. 5 shows concentration profiles, based on Eq. (3) at pH 4 and 11, at different ionic strengths. According to the general model, the diffusive flux is very dependent on the ionic strength in the range 1–10 m*M* at pH 4. The increased screening effect at ionic strengths above 10 m*M* is almost insignificant for the protein concentration studied. However, at pH 11 the diffusive flux is almost independent of ionic strength. The main reason for this independence is that the electrostatic repulsion between the lysozyme molecules is very weak, even at low ionic strengths. The effect from an increased ionic strength is therefore negligible.

Fick's law is derived with the assumption that the studied system is ideal, while the general model is valid for both ideal and non-ideal systems, since any deviations from an ideal behaviour can be included. If the two models are applied on ideal systems, they should give the same results. Fig. 6 shows concentration profiles obtained with both Fick's law and the general model at different pH and ionic strength. At pH 4 and 0.1 *M* the two models agree well. The assumption that the system can be regarded as an ideal system seems to be correct.

At pH 4 with ionic strength 0.005 *M*, the two models disagree. The profiles obtained with Fick's law are identical to those obtained at 0.1 *M*, while the profiles obtained with the general model are changed. Finally, at pH 11 with low ionic strength, the two models agree well again. This is because lysozyme has a very low charge at pH 11 and thereby the system can be regarded as ideal.

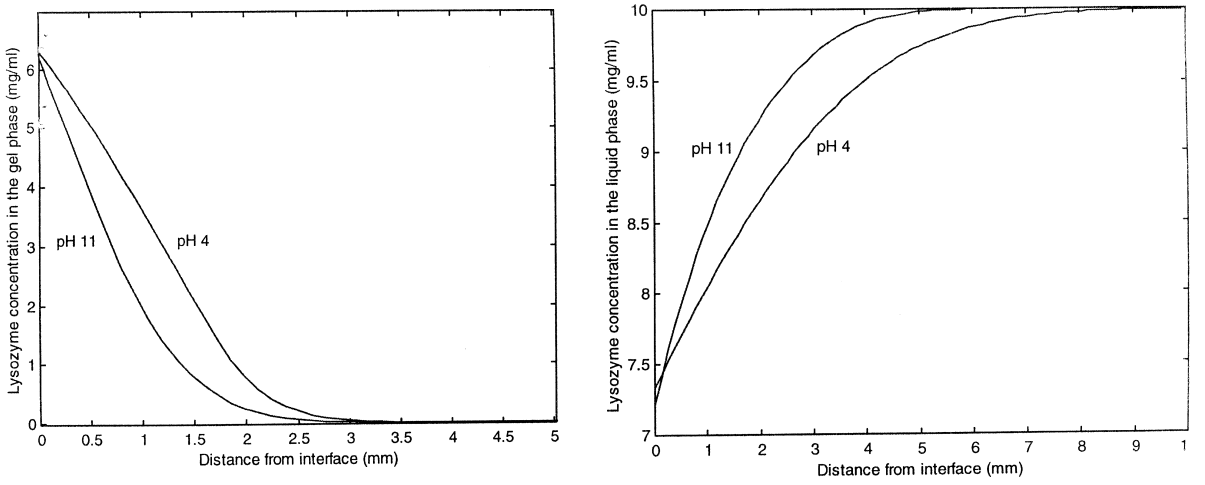

Fig. 3. Simulated concentration profiles at pH 4 and pH 11, at 0.005 *M* NaCl, in both the gel phase (left) and the liquid phase (right). $C_{10}=0$ mg/ml, $C_{20}=10$ mg/ml, $k=0.86$, $D_g=6.3\times10^{-11}$ m^2/s and $D_{liq}=12.8\times10^{-11}$ m^2/s, $t=2$ h.

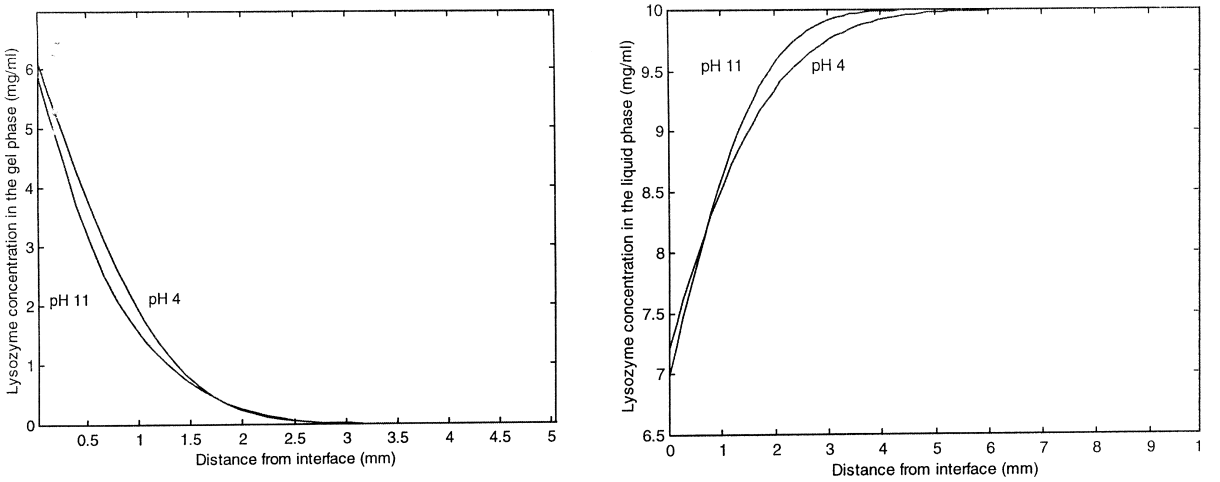

Fig. 4. Simulated concentration profiles at pH 4 and pH 11, at 0.1 *M* NaCl, in both the gel phase (left) and the liquid phase (right). $C_{10}=0$ mg/ml, $C_{20}=10$ mg/ml, $k=0.86$, $D_g=6.3\times10^{-11}$ m^2/s and $D_{liq}=12.8\times10^{-11}$ m^2/s, $t=2$ h.

5.2. Holographic laser interferometry measurements

Diffusion experiments with lysozyme were performed in two series. The first at a high ionic strength of 0.1 *M* NaCl, and the second where the protein was dissolved in distilled water. Measurements were performed within each series at pH 4, 5.6 and 11. For each experiment, several interference patterns were recorded at different times.

In Fig. 7, photographic pictures of interference patterns from three different experiments are shown. The three experiments were performed at different pH and ionic strength but with the same initial protein concentration (10 mg/ml) in the liquid phase. The experimental time was approximately the same for all three experiments. Since a tighter interference pattern represents a steeper concentration profile within both the gel and the liquid, it is easy to see how the diffusive flux varied with pH and ionic strength. At pH 4 with low ionic strength (No. 1) the diffusive flux was faster than at pH 11 with the same ionic strength (No. 3). Even at pH 4 but with high ionic strength, 0.1 *M* (No. 2), the diffusive flux was almost the same as at pH 11 with low ionic strength. The increase in ionic strength at pH 4 (No. 2) slowed down the diffusive flux. This is in agreement with the results obtained from the simulation study. The non-Fickian behaviour at pH 4 and low ionic strength can be clearly seen (No. 1) since the interference fringes appear more or less at constant distances. The Fickian behaviour is on the other hand seen in the other (Nos. 2–3) where the interference pattern is tighter close to the interface.

Experimental liquid and gel diffusion coefficients were obtained by fitting theoretical concentration profiles to the experimental profiles using MATLAB 5. The theoretical profiles were obtained from both Fick's law (Eq. 7) and the general model (Eq. 3). The only parameter in Eqs. (3) and (7) that was varied was the diffusion coefficient.

5.3. Experimental liquid diffusion coefficients

Liquid diffusion coefficients were obtained by fitting theoretical concentration profiles to experimental concentration profiles. The best fit was obtained by minimising the object function:

$$\chi^2=\sum_{z=1}^{n}\left(\left(\frac{\Delta C_z}{\Delta C_{tot}}\right)_{exp}-\left(\frac{\Delta C_z}{\Delta C_{tot}}\right)_{calc}\right)^2 \qquad (14)$$

The diffusion coefficients were evaluated using both Fick's law and the general model (GM). The liquid diffusion coefficients obtained from the fitting are presented in Table 4 for all experiments. When lysozyme was dissolved in distilled water, the ionic strength in the solution increased by a few m*M*. This

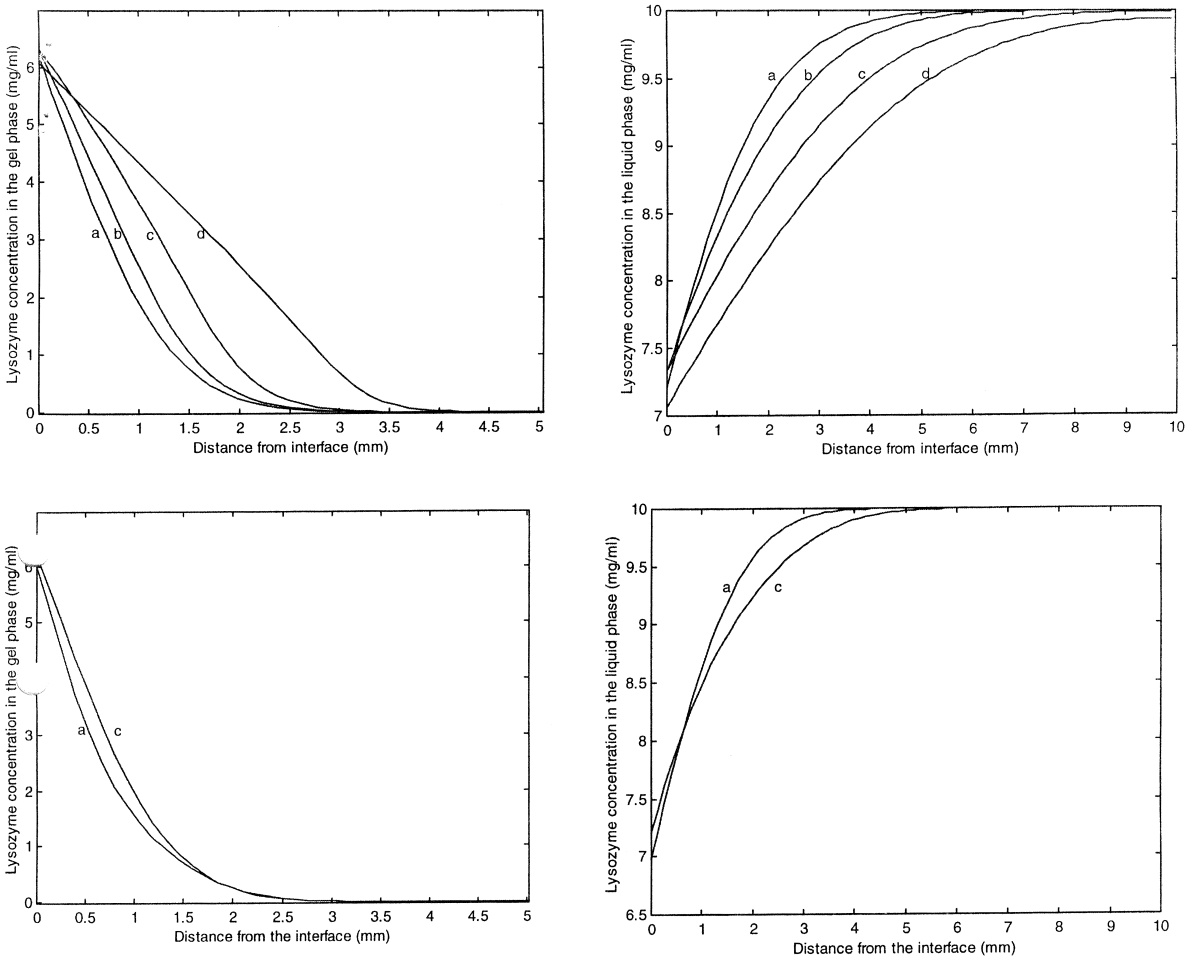

Fig. 5. Concentration profiles at different ionic strengths at pH 4 (top figures) and pH 11 (lower figures), in both the gel phase (left) and the liquid phase (right). $C_{10}=0$ mg/ml, $C_{20}=10$ mg/ml, $k=0.86$ (pH 4), $D_g=6.3\times10^{-11}$ m^2/s and $D_{liq}=12.8\times10^{-11}$ m^2/s, $t=2$ h.) Curves: (a) 0.1 *M*; (b) 0.01 *M*; (c) 0.005 *M*; and (d) 0.002 *M*.

is because the solid lysozyme contains salt ions. The pH was then adjusted by adding small amounts of HCl or NaOH. The resulting ionic strength was unknown. The chemical potential for a protein with a high charge number depends largely on the ionic strength, if the ionic strength is in the range 1–10 m*M* (for the used lysozyme concentration). This means that the driving force (the chemical potential gradient) in the general model will be ionic strength dependent. This is normally not a problem since the ionic strength is set and thereby known. In the present study the ionic strength was unknown and was set to a value such that the general model gave liquid diffusion coefficients that agreed well with literature data for lysozyme in ideal systems (Table 1).

The chemical potential as a function of concentration was calculated for different ionic strengths. These functions were then used to model the diffusion process and the model fitted to experimental data. The function that gave liquid diffusion coefficients that matched the literature data was in this way used to estimate the ionic strength. In this study the function for chemical potential obtained at an ionic strength of 5 m*M* resulted in the best agreement and was thus used to evaluate all the experi-

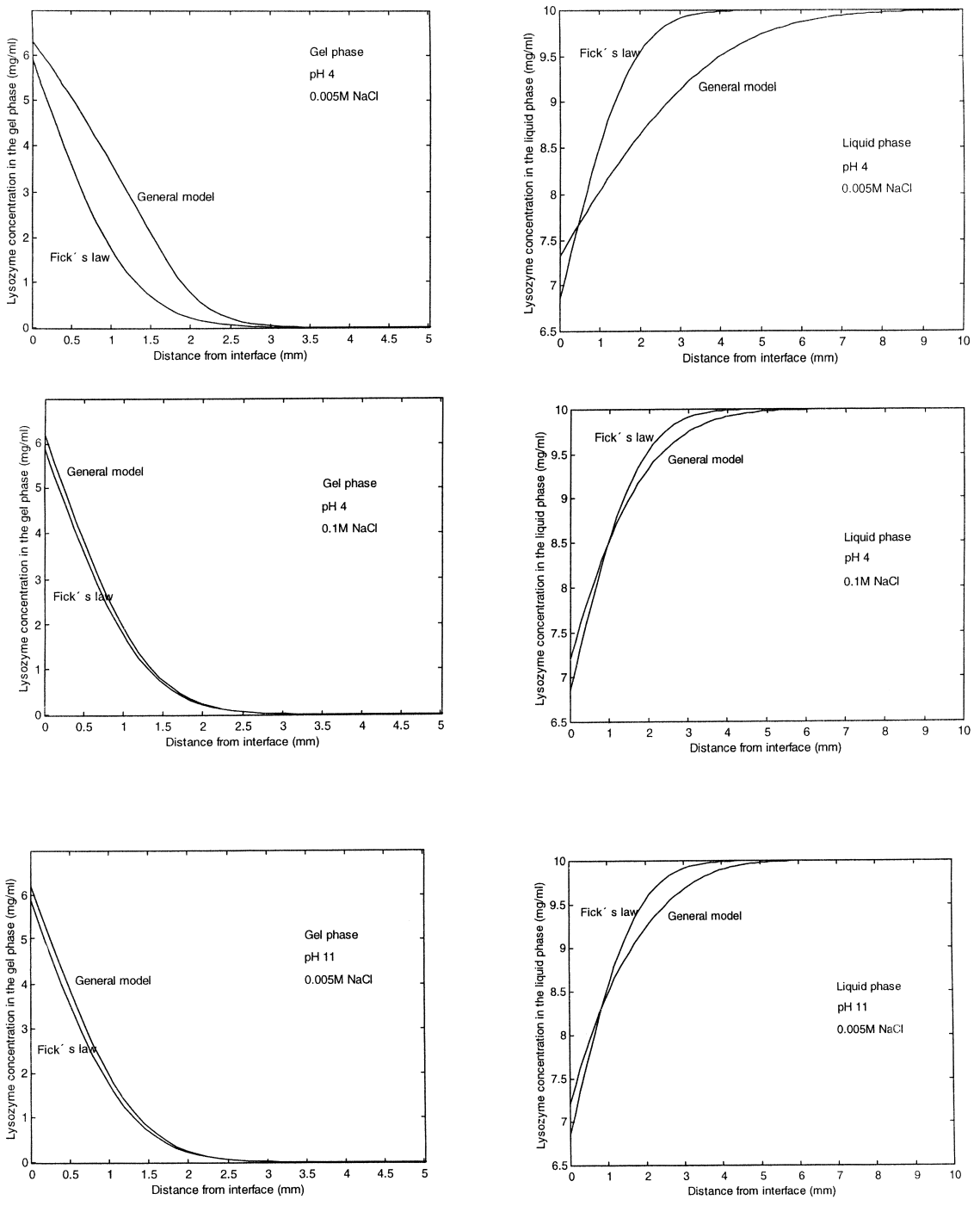

Fig. 6. Comparison between concentration profiles obtained with Fick's law and the general model at different pH and ionic strengths. $C_{10}=0$ mg/ml, $C_{20}=10$ mg/ml, $k=0.86$ (pH 4), $D_g=6.3\times10^{-11}$ m^2/s and $D_{liq}=12.8\times10^{-11}$ m^2/s, $t=2$ h.

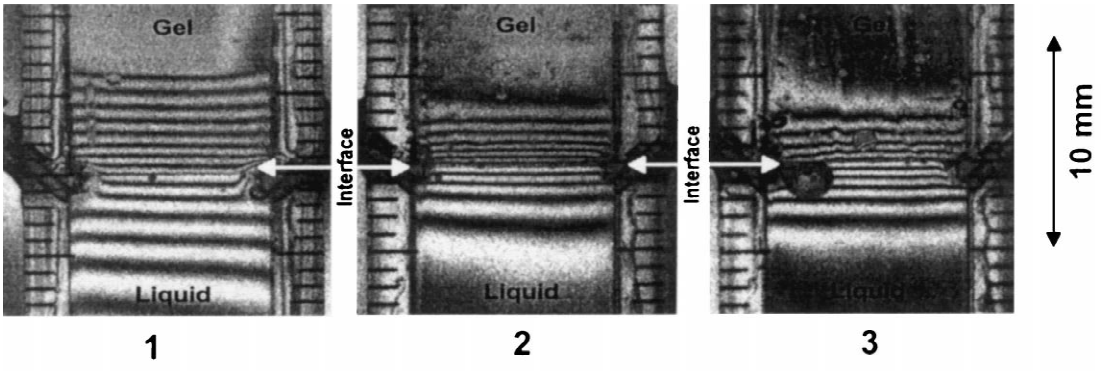

Fig. 7. Photographs of experimental interference patterns obtained with HLI. No. 1: pH 4, 0.005 *M* NaCl, $t=423$ min. No. 2: pH 4, 0.1 *M* NaCl, $t=431$ min. No. 3: pH 11, 0.005 *M* NaCl, $t=409$ min.

ments at low ionic strength. Fig. 8 shows Fick's law and the general model fitted to the experimental concentration profile in the liquid phase at pH 4, at low ionic strength (Experiment No. 6, $t=187$ min).

5.4. Experimental gel diffusion coefficients

The concentration profiles in the gel phase were evaluated using the assumption that the ionic strength was the same as in the liquid phase. The gel slabs had been equilibrated in a solution prepared in the same way, with adjusted pH, as the solution the protein had been dissolved in before each experiment. From the interference patterns in the liquid and in the gel phase it could be seen that the same trend occurred in both phases (see Fig. 7). Gel diffusion coefficients were obtained by fitting theoretical concentration profiles to experimental concentration profiles. The best fit was obtained by minimising the object function, Eq. (14).

Using Fick's law the obtained diffusion coefficients at low ionic strength were abnormally high at pH 4 and 5.6. Evaluation of the experiments at pH 4 and 5.6 using the general model, resulted in diffusion coefficients that were lower than those obtained by Fick's law but which were sometimes higher than those obtained in the liquid phase using the general model. At high ionic strength and at pH 11, both models gave diffusion coefficients that agreed well with each other.

Diffusion coefficients obtained from the fitting procedure are presented in Table 5 for all experiments. Fig. 9 shows Fick's law and the general model fitted to the experimental concentration profile in the gel phase at pH 4, at low ionic strength (Experiment No. 6 $t=187$ min).

Table 4
Liquid diffusion coefficients[a] obtained with HLI at 25°C

Exp.	Ionic strength (*M*)	pH	$D_{liqFick}$[b] (10^{-11} m^2/s)	D_{liqGM}[c] (10^{-11} m^2/s)
1	0.1	4	11.0±1.2	10.0±1.2
2	0.1	4	11.7±1.3	10.6±1.2
3	0.1	5.6	12.3±2.2	11.7±2.3
4	0.1	5.6	14.0±1.9	13.4±1.8
5	0.005	4	54.2±7.2	13.9±1.5
6	0.005	4	51.00±3.2	12.5±0.8
7	0.005	11	12.4±1.7	10.2±1.4
8	0.005	11	16.1±2.9	13.0±2.1
9	0.005	5.6	51.9±4.4	14.9±1.3
10	0.005	5.6	41.5±8.3	11.7±2.4
11	0.005	5.6	36.2±6.5	11.1±2.0

[a] Mean±standard deviation within each experiment based on several interference patterns evaluated at various times.
[b] Obtained using Ficks law.
[c] Obtained using the general model (GM).

5.5. Partition coefficients

The partition coefficients obtained are presented in Table 6. The protein net charge at pH 11 is close to zero, which makes the protein very prone to precipitate. This made it difficult to perform experiments at pH 11. In both experiments at pH 11, it was possible to detect a small amount of lysozyme that had

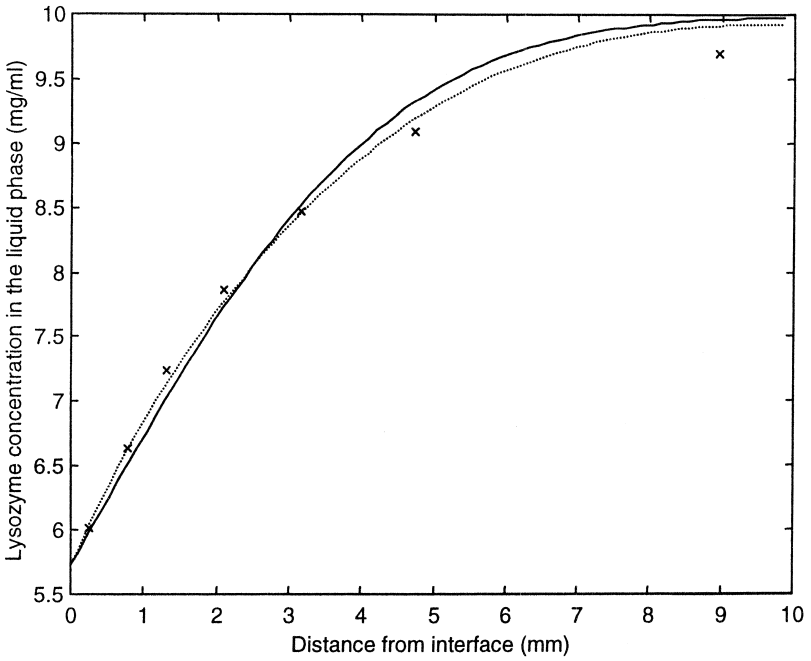

Fig. 8. Fick's law and the general model fitted to the experimental concentration profile obtained in the liquid phase after 187 min. Experiment No. 6: solid line, Fick's law; dotted line, the general model; x = experimental concentration.

precipitated. This can be one reason why the obtained partition coefficient at pH 11 is lower than at other pH values. Another possible explanation could be that since lysozyme at pH 11 is almost neutral, the molecules do not repel each other and might exist as oligomers, instead of monomers and dimers. At pH 4 and 5.6, lysozyme exists as monomers or dimers [25]. Since oligomers are larger than the

Table 5
Gel diffusion coefficients[a] obtained with HLI at 25°C

Exp.	Ionic strength (M)	pH	D_{gFick}[b] (10^{-11} m^2/s)	D_{gGM}[c] (10^{-11} m^2/s)	D_{gGM}[c] (10^{-11} m^2/s), ionic strength 0.002
1	0.1	4	9.10±1.4	8.4±1.5	–
2	0.1	4	8.8±0.6	8.2±0.5	–
3	0.1	5.6	8.00±0.5	7.5±0.5	–
4	0.1	5.6	7.4±0.5	6.9±0.5	–
5	0.005	4	33.00±2.1	16.5±1.3	7.21±0.6
6	0.005	4	32.4±1.2	15.2±0.5	6.8±0.2
7	0.005	11	8.5±1.0	8.1±1.0	8.1±1.0
8	0.005	11	9.3±0.9	9.0±0.9	9.0±0.9
9	0.005	5.6	34.5±1.7	15.8±0.6	8.3±0.4
10	0.005	5.6	28.0±2.9	13.4±1.3	6.3±0.5
11	0.005	5.6	25.2±2.2	13.7±1.3	6.3±0.60

[a] Within each experiment several interference patterns were evaluated and hence the value presented here is the mean±standard deviation.
[b] Obtained using Fick's law.
[c] Obtained using the general model (GM).

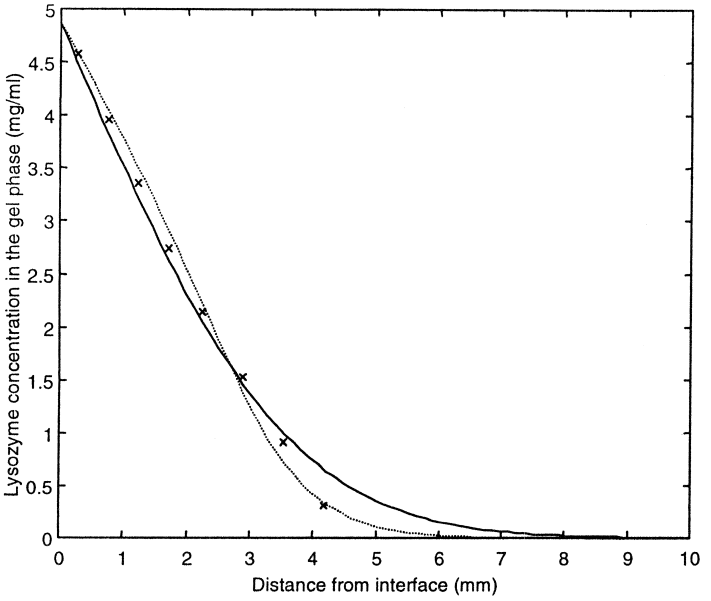

Fig. 9. Fick's law and the general model fitted to the experimental concentration profile obtained in the gel phase after 187 min, experiment No. 6. Solid line = Fick's law, dotted line = the general model, x = experimental concentration..

monomers and the dimers, they might be more restricted by the polymer network in the gel.

The partition coefficients obtained here were of the same size or slightly lower than the one used in the simulation study ($k = 0.86$ [24]). The volume fraction of polymer in Vonk's study [24] was lower than the polymer fraction in this study. A higher polymer fraction should result in lower partition coefficients and hence the trend in this study seems correct. However, except for Experiments 7 and 8 the obtained partition coefficients overlap each other. Any conclusions about the influence of pH and ionic strength can therefore not be made.

Table 6
Partition coefficients[a], k, and the ratio D_g/D_{liq} obtained with HLI

Exp.	Ionic strength (M NaCl)	pH	k	D_g/D_{liq} [b]	D_g/D_{liq} [c]
1	0.1	4	0.71±0.05	0.83	0.84
2	0.1	4	0.75±0.05	0.75	0.77
3	0.1	5.6	0.84±0.05	0.65	0.64
4	0.1	5.6	0.95±0.05	0.53	0.51
5	0.005	4	0.70±0.05	0.61	1.19
6	0.005	4	0.81±0.05	0.63	1.22
7[d]	0.005	11	0.50±0.04	0.68	0.79
8[d]	0.005	11	0.38±0.02	0.58	0.69
9	0.005	5.6	0.76±0.04	0.68	1.06
10	0.005	5.6	0.80±0.05	0.68	1.15
11	0.005	5.6	0.80±0.05	0.69	1.23

[a] Best estimated value±maximum deviation.
[b] Gel diffusion coefficients obtained with Fick's law.
[c] Gel diffusion coefficients obtained with the general model (GM).
[d] Small amounts of lysozyme have precipitated.

The total number of fringes in each phase is set by the concentration difference between the interface and the unaffected part of the phase (top/bottom). The concentration at the unaffected part of each phase is constant and equal to the start concentrations. Therefore, if the concentration at the interface in each phase is also constant, then the total number of fringes during an experiment should be constant.

It was observed that the total number of fringes in each phase was constant during an experiment, as long as the diffusion process was stopped before it reached the end of any of the phases. This was observed in all experiments, not only in those with high ionic strength that behave ideally, but also in the experiments with low ionic strength and non-ideal behaviour.

6. Discussion

6.1. Experimental liquid diffusion coefficients

At pH 4 and low ionic strength, the obtained diffusion coefficients of lysozyme in liquid differed significantly depending on which model was used for evaluation (Table 4). Using Fick's law resulted in abnormally high diffusion coefficients, while the general model gave more probable values according to the literature. At pH 4 and 0.1 *M* ionic strength the diffusion coefficients obtained from the two models agreed well and were in the same range as the diffusion coefficient obtained at low ionic strength with the general model.

The same trend could be seen at pH 5.6, but the very high diffusion coefficients obtained with Fick's law were slightly lower than at pH 4, which seems reasonable since lysozyme has a lower charge at pH 5.6 than at pH 4. At pH 11, both models gave approximately the same diffusion coefficients, which are similar to those obtained at pH 4 and 5.6, with high ionic strength.

The results show that if Fick's law is used to describe the diffusion process, then the obtained diffusion coefficient varies with pH and ionic strength, while the general model gives a diffusion coefficient that is independent of pH, if the ionic strength is known.

6.2. Experimental gel diffusion coefficients

All gel diffusion coefficients obtained at 0.1 *M* NaCl were higher than the gel diffusion coefficients used in the simulation study (6.3×10^{-11} m^2/s [24]). This is surprising since the volume fraction polymer in this study is higher than in the study by Vonk [24]. However, Vonk [24] obtained the diffusion coefficients indirectly by using chromatography experiments. Diffusion coefficients obtained by chromatography are based on equations that contain several physical constants. These constants have to be known or determined experimentally at the same time as the diffusion coefficient is determined. To determine diffusion coefficients using holographic laser interferometry, only the partition coefficient has to be known. Therefore, the difference between the two methods can be a possible explanation for the difference between the values obtained here and the one obtained by Vonk [24].

The gel diffusion coefficients obtained with the general model were almost as high, and sometimes even higher (Table 5), as those in the liquid phase. From the picture in Fig. 7 the reverse was expected, i.e., a lower diffusion coefficient in the gel since diffusion in the gel phase is hindered. The simulation results showed that the diffusive flux was ionic strength dependent for charged molecules.

One possible explanation could be that the polymer network in the gel phase interacts with the charged lysozyme molecules. Not only lysozyme–lysozyme interactions but also lysozyme–gel interactions affect the diffusion process. Using Poisson–Boltzmann's equation it is possible to calculate the electrostatic interaction energy as a function of the distance between one lysozyme molecule and a plane surface [26]. The surface can be either charged or neutral. Fig. 10 shows the electrostatic interaction energy as a function of the distance between a lysozyme molecule and a neutral surface at differing pH and ionic strength.

One interpretation of the curves is that the energy required to push a lysozyme molecule towards the neutral surface is inversely related to the distance between the molecule and the surface. This means that it is not probable that any lysozyme molecule will be found close to the surface. The probability of finding a molecule at a certain distance is given by $e^{(\text{electrostatic interaction energy})}$ (Fig. 11). Assuming that no lysozyme molecule will be found until the probability is almost 1, gives that there will be no molecules closer to the surface than 70 Å (at pH 4 and 0.005 m*M* NaCl). If a cylindrical geometry is assumed as a simplified description of an agarose pore, it is possible to calculate how much the accessible volume decreases due to the interaction forces. Using an average pore diameter of 400 Å for 4% agarose [27] (where the accessible pore diameter for a lysozyme molecule is 400 Å $-2\times$ lysozyme radius (Fig. 11)) and subtracting 2×70 Å results in a decrease in accessible volume of 48%. This would lead to an increase in protein concentration by a factor of 2 in the 'accesible' pore liquid. The increase in concentration results in a higher chemical potential in the 'accessible' pore liquid and hence increased driving force for the diffusive flux.

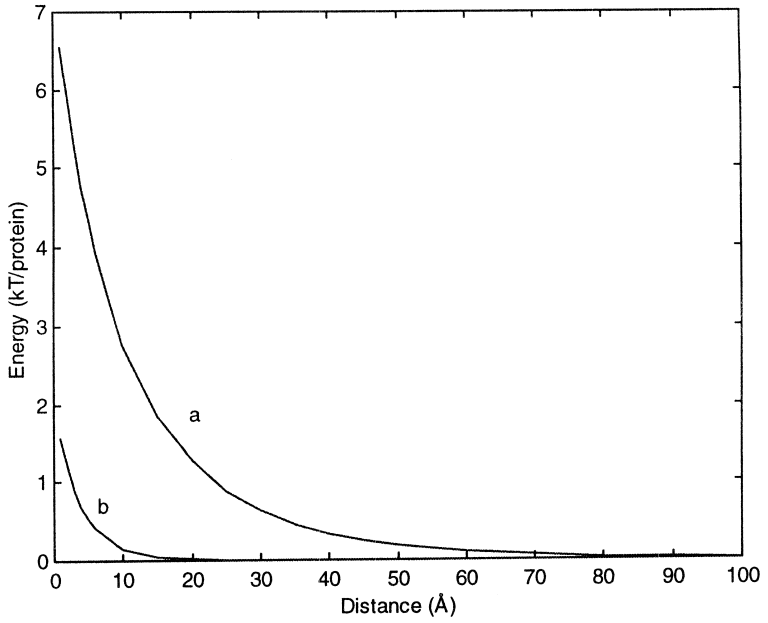

Fig. 10. Interaction energy as a function of the separation distance between a planar uncharged surface and a charged lysozyme molecule at $T=298$ K. Curves: (a) pH 4, 0.005 *M* NaCl; (b) pH 4, 0.1 *M* NaCl.

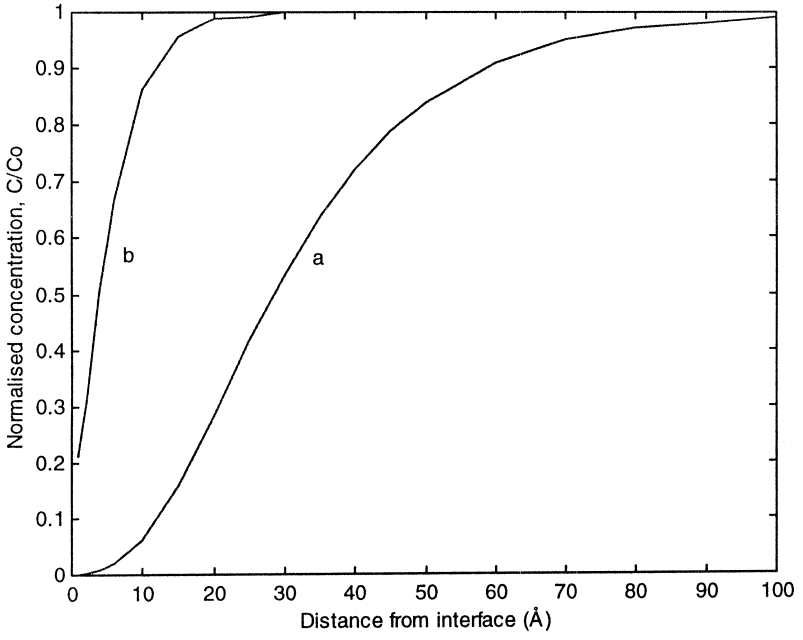

Fig. 11. The probability to find a lysozyme molecule as a function of the distance from the planar uncharged surface at $T=298$ K. Curves: (a) pH 4, 0.005 *M* NaCl; (b) pH 4, 0.1 *M* NaCl.

Another more possible explanation could be that the ionic strength is lower in the gel phase than in the liquid phase. Evaluating the gel phase by assuming ionic strengths lower than 5 m*M* gives lower diffusion coefficients, and at 2 m*M* the diffusion coefficients agree well with those obtained at 0.1 *M* (Table 5). Since the used lysozyme powder contains salt it is possible that the ionic strength in the solution is higher than in the gel.

It is also probable that the obtained high diffusion coefficients are a combined effect of the lower ionic strength in the gel phase and the lysozyme fibre interaction in the gel phase.

a	activity (mol/m^3)
b	diffusion cell thickness (m)
C_1	concentration of protein in the gel phase (mg/ml)
C_2	concentration of protein in the liquid phase (mg/ml)
C_{10}	initial concentration of protein in the gel phase (mg/ml)
C_{20}	initial concentration of protein in the liquid phase (mg/ml)
$C_{1,eq}$	equilibrium concentration of protein in the gel phase (mg/ml)
$C_{2,eq}$	equilibrium concentration of protein in the liquid phase (mg/ml)
C_{int}	concentration of protein at the interface (mg/ml)
$C_{x=\infty}$	concentration of protein at $x=\infty$ (mg/ml)
c	concentration (mol/m^3)
c_j	concentration (mol/m^3)
$c_{j(bulk)}$	bulk concentration (mol/m^3)
D	diffusion coefficient (m^2/s)
D_{eff}	effective diffusion coefficient (m^2/s)
D_g	gel diffusion coefficient in the gel phase (m^2/s)
D_{liq}	liquid diffusion coefficient for lysozyme (m^2/s)
D_2	diffusion coefficient in the liquid phase (m^2/s)
F	Faraday's constant (As)
$\mathbf{F}_t$	force (N)
J	flux (mol/m^2s)
k	partition coefficient (–)
n	refractive index (–)
P	pressure (N/m^2)
q	charge (As)
R	universal gas constant (J/mol K)
r	distance (m)
S_i	molar entropy (J/mol K)
T	temperature (K)
t	time (s)
V	molar volume (m^3)
x	distance from the gel–liquid interface (m)
z	charge number (–)
ΔC_{tot}	total change in concentration between the interface and the unaffected part of the gel/liquid phase (mg/ml)
ΔC_z	change in concentration between fringe z and the unaffected part of the gel/liquid phase (mg/ml)
ε_o	permittivity of vacuum (As/Vm)
ε_r	dielectric constant of the solvent used (–)
μ	chemical potential (J/mol)
$\mu_{i,el}$	long-range electrostatic interactions (J/mol)
Δn	change in refractive index (–)
Δx	change in length (m)
λ	wavelength in air for the laser light (m)
Ψ	electrostatic potential (V)

Acknowledgements

The financial support from the Swedish Centre for Bioseparation is gratefully acknowledged. Dr Philippe Roger gratefully acknowledges the financial support of the European Communities, grant FAIR-CT965072.

References

[1] L. Stryer, in: Biochemistry, 3rd Edition, W.H. Freeman, New York, 1988.
[2] J.A. Wesselingh, R. Krishna, in: Mass Transfer, Ellis Horwood, Chichester, 1990.
[3] B.D. Fair, D.Y. Chao, A.M. Jamieson, J. Colloid Interface Sci. 66 (2) (1978) 323.
[4] A.K. Gaigalas, J.B. Hubbard, M. McCurley, S. Woo, J. Phys. Chem. 96 (1992) 2355.

[5] D.G. Leaist, J. Phys. Chem. 93 (1989) 474.
[6] B. Nyström, R.M. Johnsen, Chem. Scripta 22 (1983) 82.
[7] T. Raj, W.H. Flygare, Biochemistry 13 (16) (1974) 3336.
[8] R.E. Cameron, M.A. Jalil, A.M. Donald, Macromolecules 27 (1994) 2708.
[9] N. Bochner, J. Pipman, J. Phys. D: Appl. Phys. 9 (1976) 1825.
[10] H. Fenichel, H. Frankena, F. Groen, Am. J. Phys. 52 (1984) 735.
[11] M. Gierow, Å. Jernqvist, Measurement of mass diffusivity with holographic interferometry for H_2O/NaOH and H_2O/LiBr working pair, in: Proceedings of the Int Absorption Heat Pump Conference, 1993, p. 525.
[12] N.O. Gustafsson, B. Westrin, A. Axelsson, G. Zacchi, Biotechnol. Prog. 9 (1993) 436.
[13] D.D. Kong, T.F. Kosar, R.S. Dungan, R.J. Phillips, AIChE J. 43 (1) (1997) 25.
[14] C. Mattisson, T. Nylander, A. Axelsson, G. Zacchi, Chem. Phys. Lipids 84 (1996) 1.
[15] F. Ruiz-Beviá, A. Celdran-Mallol, C. Santos-Garcia, J. Fernández-Sempere, Can. J. Chem. Eng. 63 (1985) 765.
[16] F. Ruiz-Beviá, J. Fernández-Sempere, J. Colom-Valiente, AIChE J. 35 (11) (1989) 1895.
[17] J. Szydlowska, B. Janowska, J. Phys. D: Appl. Phys. 15 (1982) 1385.
[18] B. Westrin, Diffusion Measurements in Gels: A Methodological Study. Ph.D. Thesis, Lund University, Lund, Sweden, 1991.
[19] P. Roger, A. Axelsson, C. Mattisson, G. Zacchi, Report, Department of Chem. Eng. 1, University of Lund, LUTKDH/(TKKA-7002)/1-29/(1998) 1998.
[20] P.W. Atkins, in: Physical Chemistry, 1st Edition, Oxford University Press, London, 1978.
[21] A. Jönsson, B. Jönsson, J Colloid Interface Sci. 180 (1996) 504.
[22] B. Mörnstam, K.G. Wahlund, B. Jönsson, Anal. Chem. 69 (1997) 5037.
[23] J. Crank, in: The Mathematics of Diffusion, Oxford University Press, Oxford, 1975.
[24] P. Vonk, Diffusion of Large Molecules in Porous Structures. Ph.D Thesis, Rijksuniversiteit Groningen, The Netherlands, 1994.
[25] R.M. Bruzzesi, E. Chiancone, E. Antonini, Biochemistry 4 (9) (1965) 1796.
[26] J. Ståhlberg, U. Appelgren, B. Jönsson, J. Colloid Interface Sci. 176 (1995) 397.
[27] A. Medin, Studies on structure and Properties of Agarose, Ph.D. Thesis, Uppsala University, Uppsala, Sweden, 1995.
[28] C. Bor Fuh, S. Levin, J.C. Giddings, Anal. Biochem. 208 (1993) 80.
[29] S.B. Dubin, J.H. Lunacek, G.B. Benedek, Physics 57 (1967) 1164.
[30] M.K. Liu, P. Li, J.C. Giddings, Protein Sci. 2 (1993) 1520.
[31] PBCell, Web-site address: http://www.membfound.lth.se/chemeng1.html